PHYSICAL REVIEW B VOLUME 18, NUMBER 11 1 DECEMBER 1978

Quasiparticle and phonon propagation in bulk, superconducting lead

V. Narayanamurti, R. C. Dynes, P. Hu, H. Smith,* and W. F. Brinkman
Bell Laboratories, Murray Hill, New Jersey 07974
(Received 2 August 1978)

We present a detailed account of our work on the propagation of quasiparticles and phonons in bulk, superconducting lead. Time-of-flight techniques combined with tunnel junction detection (for quasiparticles) and bolometer detection (for phonons) are used. A transition from quasiparticle diffusion (and ballistic phonon propagation) to diffusion in the combined gas of quasiparticles and phonons is observed as the temperature is increased. We give a theoretical description of the pulse propagation characteristics in the diffusive regimes. The theoretical line-shape fits to the data yield a measure of the quasiparticle recombination time and their number decay time as a function of temperature.

I. INTRODUCTION

Recently, there has been considerable activity in the study of nonequilibrium superconductivity.[1] Most of the experimental studies to data have involved the study of the superconducting transition of a thin film or the I-V characteristics of a thin-film tunnel junction. In a recent paper,[2] we reported on the propagation characteristics of photoexcited quasiparticles in bulk, single-crystal, superconducting lead using a tunnel junction as a quasiparticle detector and time-of-flight techniques with nanosecond resolution. The combined use of bulk samples and time-of-flight techniques made possible a direct determination of the spatial and temporal behavior in the nonequilibrium state in a previously unexplored regime.

In this paper we present a full experimental and theoretical account of this work. We shall first discuss the various characteristic times that are important in the temperature range under consideration (Sec. II). We show that the relaxation time for the decay of the excess number of quasiparticles may be very long, this being the key to the understanding of the observed diffusive behavior of the quasiparticles and phonons. In Sec. III we present the coupled diffusion equations for quasiparticles and phonons, and discuss their justification. We solve the equations for a point source in an infinite medium, and show how these solutions are modified in a finite slab. In Secs. IV and V we discuss the experimental techniques and results. In Sec. VI we make a detailed comparison of theory and experiment.

II. CHARACTERISTIC TIMES

An extensive study of various characteristic times of a superconductor has recently been reported by Kaplan *et al.*[3] Since we are interested in temperatures well below the gap Δ, it is convenient to use the low-temperature ($k_BT \ll \Delta$) expressions for these quantities in our subsequent discussion. For this purpose we use a form of the electron-phonon matrix element g_q that emphasizes its low-temperature properties,

$$|g_q|^2 = \lambda\hbar\omega/2N(0)\,, \tag{2.1}$$

where $\hbar\omega$ is the phonon energy and $2N(0)$ the density of states for both spins at the Fermi surface of the normal metal. The constant λ (which is of order unity) determines the mass enhancement through $m^* = m(1+\lambda)$, if the q dependence of the electron-ion pseudopotential is neglected. When we need the magnitude of the scattering rates for a given metal, we employ the relation

$$\alpha^2F(\omega) = \lambda(\hbar\omega)^2/4(k_B\Theta)^2\,, \tag{2.2}$$

where $\alpha^2F(\omega)$ is the usual effective-phonon density of states used in Ref. 3. The scattering Debye temperature Θ is here defined as $k_B\Theta = p_Fc$ with c the sound velocity and p_F the Fermi momentum.

For purposes of the following discussion we summarize the results of the standard golden-rule calculation of the normal-state relaxation rate $\tau_N^{-1}(0)$ at the transition temperature T_c and at the Fermi energy, the low-temperature scattering rate τ_S^{-1} of a quasiparticle at the gap edge, and the low-temperature recombination rate τ_R^{-1} of a quasiparticle at the gap edge. The expressions may be written (with $\hbar = k_B = 1$)

$$1/\tau_N(0) = \tfrac{7}{2}\pi\zeta(3)\lambda T_c^3/\Theta^2\,, \tag{2.3}$$

$$1/\tau_S = (15\pi^{3/2}/16\sqrt{2})\zeta(\tfrac{7}{2})\lambda T^{7/2}/\Theta^2\Delta^{1/2}\,, \tag{2.4}$$

where $\zeta(n)$ denotes the ζ function, and

$$1/\tau_R = (2\pi)^{3/2}\lambda(\Delta^{5/2}T^{1/2}/\Theta^2)e^{-\Delta/T}\,. \tag{2.5}$$

The numerical coefficients in front of these expressions are close to 13, 4, and 16, respectively. Since

$$\tau_R/\tau_S = 0.3(T^3/\Delta^3)e^{\Delta/T}\,, \tag{2.6}$$

the scattering rate is seen to be larger than the

recombination rate below a temperature $T \simeq \Delta/6 \simeq 2.7$ K, when the value $\Delta = 16.3$ K appropriate for lead is used for the zero-temperature gap.

With the identification $1/\tau_N(0) = 7\zeta(3)(1/\tau_0)$, we may extract the normal-state relaxation rate $1/\tau_N(0)$ at T_c from τ_0 as defined and tabulated in Ref. 3. For Pb we get

$$1/\tau_N(0) = 4 \times 10^{10}\ \text{sec}^{-1}. \tag{2.7}$$

Using the zero-temperature gap value $\Delta = 2.26\ T_c$, we then obtain

$$1/\tau_S = 0.2(T/T_c)^{7/2}[1/\tau_N(0)], \tag{2.8}$$

$$1/\tau_R = 9(T/T_c)^{1/2} e^{-2.26 T_c/T}[1/\tau_N(0)], \tag{2.9}$$

which is a convenient estimate of the magnitude of the scattering rates at a given reduced temperature $t = T/T_c$ in the low-temperature region ($t \lesssim \frac{1}{2}$). We stress that these expressions do not take into account strong-coupling corrections to α^2F, which for Pb are numerically important for the recombination rate, as shown in Ref. 3. For an accurate comparison between theory and experiment one must use for τ_R the general expression given in Ref. 3 [Eq. (15)].

Turning now to the role of impurity scattering we may estimate the normal-state impurity relaxation rate τ_{imp} in a free-electron model to be

$$1/\tau_{\text{imp}} \simeq 5 \times 10^9\ \text{sec}^{-1} \tag{2.10}$$

for a Pb sample with resistance ratio of 20 000. As a consequence, the impurity scattering rate dominates the rates $1/\tau_R$ and $1/\tau_S$ at temperatures below 2 K. In this regime we therefore expect the diffusion of quasiparticles to be limited by impurity scattering.

Let us briefly discuss the role of electron-electron scattering as a possible additional scattering mechanism. For Pb one expects it to be totally unimportant, as confirmed by the following estimate, but we shall give the results of a more detailed calculation to elucidate its possible importance for a metal like Al. The estimate indicates that one does not expect to see effects of electron-electron scattering even for Al, since the electron-phonon interaction always dominates the inelastic part of the total scattering.

To obtain the low-temperature electron-electron limited relaxation rate we use the results of Pethick, Smith, and Bhattacharyya[4] for quasiparticle scattering in ^{3}He at low temperatures. Their result is in the present notation

$$\left(\frac{1}{\tau}\right)_{\text{qp-qp}} = \frac{\pi^2}{6}\Delta\frac{n_{\text{ex}}}{n}\left(\frac{1}{2\pi}[2N(0)]^2\langle w_S\rangle\right), \tag{2.11}$$

where n_{ex}/n is the number of excitations n_{ex} relative to the total particle number n in the (isotropic) superfluid state. The quantity in brackets is a dimensionless number that involves the collision probability w_S in the superfluid state. The normal-state relaxation rate $[1/\tau_N(0)]_{e\text{-}e}$ may be written, in a similar fashion,

$$\left(\frac{1}{\tau_N(0)}\right)_{e\text{-}e} = \frac{\pi^3}{16}\frac{T_c^2}{T_F}\left(\frac{1}{2\pi}[2N(0)]^2\langle w_N\rangle\right). \tag{2.12}$$

The ratio of the rates is

$$\frac{(1/\tau)_{\text{qp-qp}}}{[1/\tau_N(0)]_{e\text{-}e}} = \frac{8}{3\pi}\frac{\Delta T_F}{T_c^2}\frac{n_{\text{ex}}}{n}\frac{\langle w_S\rangle}{\langle w_N\rangle}. \tag{2.13}$$

For an interaction that has a constant spin singlet amplitude (and zero triplet), the ratio $\langle w_S\rangle/\langle w_N\rangle$ may be shown to equal $\frac{7}{15}$.[4] Such an interaction is not an altogether unreasonable approximation to a screened Coulomb interaction; in any case, one does not expect the ratio to differ significantly from unity for a more realistic interaction. Putting in this estimated value of $\langle w_S\rangle/\langle w_N\rangle$, we obtain a formula similar to Eq. (9),

$$\frac{(1/\tau)_{\text{qp-qp}}}{[1/\tau_N(0)]_{e\text{-}e}} = 3\left(\frac{T}{T_c}\right)^{1/2} e^{-\Delta/T}, \tag{2.14}$$

where we have kept the zero-temperature gap Δ in the exponential in order that the estimate may apply to cases of weak and strong coupling.

To estimate $[1/\tau_N(0)]_{e\text{-}e}$, we use the results of the Born approximation which for a screened Coulomb potential may be shown to be accurate to within a factor of 2 when the resulting scattering rate is compared to the one obtained by a phase-shift calculation.[5] For an r_S value equal to 2 (characterizing both Pb and Al) the relaxation rate for an electron at the Fermi energy becomes

$$[(1/\tau_N(0)]_{e\text{-}e} = 1.6 \times 10^6 T_c^2\ \text{sec}^{-1}, \tag{2.15}$$

where the transition temperature T_c is measured in kelvin.

For Pb, (2.15), yields a value of $1/\tau_N(0) = 9 \times 10^7$ sec^{-1}, which makes the contribution of electron-electron scattering in the normal state as well as in the superconducting state totally negligible. For Al the electron-electron scattering rate at T_c becomes 2×10^6 sec^{-1}, which is considerably smaller than that due to electron-phonon interaction, which gives $1/\tau_N(0) = 2 \times 10^7$ sec^{-1}. Comparing (2.9) and (2.14), we conclude that the quasiparticle-quasiparticle scattering rate at low temperatures is a factor of 30 less than the electron-phonon recombination rate in Al. We do not, therefore, expect to be able to see effects of electron-electron scattering at any temperature even in metals with a Debye temperature as high as that of Al.

Finally, we discuss the rate of relaxation of an excess number of quasiparticles at low tempera-

tures. Of the various relaxation processes considered we note that both impurity scattering and scattering against phonons conserve the number of quasiparticles. The recombination processes by themselves do, of course, change the number of quasiparticles. However, the 2Δ phonon created in a recombination process may in turn create new quasiparticles, so the effective number decay time τ_{eff} becomes much longer than τ_R. Occasionally, a 2Δ phonon may break up into two other phonons via umklapp or anharmonic processes, which results in τ_{eff} being given roughly by

$$\tau_{eff} = \tau_R(\tau_{ph\to 2ph}/\tau_B), \tag{2.16}$$

where τ_B^{-1} is the rate at which a 2Δ phonon creates quasiparticles, and $\tau_{ph\to 2ph}^{-1}$ the rate at which a phonon breaks up into two other phonons. For Pb we use the estimate in Ref. 3,

$$\tau_B^{-1} \simeq 3\times 10^{10}\ \text{sec}^{-1}. \tag{2.17}$$

The rate at which the 2Δ phonon may break up into two phonons of lesser energy is not known theoretically, but we may obtain a crude estimate of its magnitude in Pb from measurements of phonon-scattering processes in Bi by Narayanamurti, Dynes, and Andres.[6] For temperatures below about 4.5 K the normal processes are dominant, while at higher temperatures umklapp (U) processes take over. In a heat pulse experiment the maximum in the phonon energy occurs at a value of about $3.8\ k_BT$. Thus the appropriate heat pulse temperature for a 2Δ phonon of energy 33 K is ~9 K. If one chooses a U-process value for $\tau_{ph\to 2ph}$, then one obtains a value of $\tau_{eff} \sim 15\ \tau_R$.

In order to investigate the possible influence of higher-order scattering processes, we have considered quantitatively the rate of a process in which two quasiparticles combine to form a phonon, subsequently breaking up into two other phonons. When the state of the intermediate phonon is broadened in accordance with the rate at which it may create quasiparticles, the rate of the entire process is similar to τ_{eff}^{-1} as given by (2.16). Clearly, a variety of higher-order processes in the combined gas of quasiparticles and phonons might be considered. Though the precise mechanism of elongation may be difficult to verify, we believe that the answer (2.16) is qualitatively correct. In Sec. III we shall study the coupled diffusion equations for the quasiparticles and phonons, and demonstrate the physical importance of the elongation of τ_R into τ_{eff}.

III. DIFFUSION OF QUASIPARTICLES AND PHONONS

In this section we formulate the coupled diffusion equations, which describe the propagation of quasiparticle and phonon pulses in the crystal. Our approach differs from the customary one only in that we allow for the possibility of separate diffusion of the excess number of quasiparticles and the local phonon temperature through introduction of relaxation terms in the diffusion equation. These relaxation terms lead to coupling of the diffusive pulses for quasiparticles and phonons at higher temperatures, but when the temperature is sufficiently low the two pulses become decoupled with a resultant large shift in the arrival time of the quasiparticle pulse. This we propose as the mechanism behind the observed transition described in Sec. V.

Though the diffusion of quasiparticles involves their excess number δn, we shall for convenience express this in terms of an equivalent change in temperature δT_e (e stands for quasiparticles, p for phonons). We write

$$\delta n = \frac{\partial n_{ex}}{\partial T}\,\delta T_e$$

for the deviation from absolute equilibrium of the total number of quasiparticles. Here n_{ex} denotes the equilibrium number of excitations introduced in Sec. II. Locally the temperature of the phonons may vary by an amount δT_p. The excess number of quasiparticles relaxes to the local equilibrium given by the number of quasiparticles appropriate to the change in local temperature δT_p. The relaxation term consequently involves

$$\delta n_{loc} = \frac{\partial n_{ex}}{\partial T}(\delta T_e - \delta T_p),$$

which differs from zero when $\delta T_e \neq \delta T_p$. We may now write the coupled diffusion equations in terms of the temperatures T_e and T_p. The left-hand side of the equations have the usual form describing heat diffusion,

$$\left(C_e\frac{\partial}{\partial t} - \kappa_e\nabla^2\right)T_e = -C_e\frac{1}{\tau_e}(T_e - T_p),$$
$$\left(C_p\frac{\partial}{\partial t} - \kappa_p\nabla^2\right)T_p = -C_p\frac{1}{\tau_p}(T_p - T_e), \tag{3.1}$$

where C is the specific heat for either system and κ the thermal conductivity. The times τ_e and τ_p are relaxation times for the electrons (quasiparticles) and phonons, respectively. From detailed balance we have

$$C_e/\tau_e = C_p/\tau_p \equiv 1/\tau, \tag{3.2}$$

where τ is expressed in units of time/(specific

heat). In the limit when $T_e = T_p = T$, which we shall show is appropriate for somewhat higher temperatures, the addition of the Eqs. (3.1) yields the usual diffusion equation describing the time and space variation of the temperature T,

$$(C_e + C_p)\frac{\partial T}{\partial t} + (\kappa_e + \kappa_p)\nabla^2 T = 0 . \tag{3.3}$$

From this we derive the diffusion coefficient

$$D = (\kappa_e + \kappa_p)/(C_e + C_p) . \tag{3.4}$$

Since at low temperatures $C_e \ll C_p$, and $\kappa_e \gg \kappa_p$, the diffusion coefficient D is to a good approximation

$$D = \kappa_e/C_p = (C_e/C_p)D_e , \tag{3.5}$$

where the quasiparticle diffusion coefficient D_e is

$$D_e = \kappa_e/C_e . \tag{3.6}$$

Evidently D_e is the diffusion coefficient appropriate for the separate diffusion of the quasiparticle gas. When the impurity scattering dominates, we have

$$\kappa_e = \tfrac{1}{3} C_e \langle v^2 \rangle \tilde{\tau}_{\rm imp} , \tag{3.7}$$

where we have written the thermal conductivity in a convenient kinetic form involving the thermally averaged square of the quasiparticle group velocity $\langle v^2 \rangle$ and an effective impurity scattering time $\tau_{\rm imp}$. At the transition temperature $\langle v^2 \rangle = v_F^2$ and $\tilde{\tau}_{\rm imp} = \tau_{\rm imp}$, while at temperatures well below the gap, $T \ll \Delta$, one has $\langle v^2 \rangle \simeq (T/\Delta) v_F^2$ and $\tilde{\tau}_{\rm imp} \simeq (2\Delta/\pi T)^{1/2} \tau_{\rm imp}$. Thus in the low-temperature range of interest $\tilde{\tau}_{\rm imp}$ differs from $\tau_{\rm imp}$ by a factor of roughly 2. Consequently, the quasiparticle diffusion coefficient becomes

$$D_e = \tfrac{1}{3} \langle v^2 \rangle \tilde{\tau}_{\rm imp} . \tag{3.8}$$

At somewhat higher temperatures, where the combined gas of quasiparticles and phonons diffuses as one pulse, the diffusion coefficient is

$$D = \tfrac{1}{3}(C_e/C_p)\langle v^2 \rangle \tau^* , \tag{3.9}$$

where $(\tau^*)^{-1}$ represents whatever relaxation rate that dominates the scattering of quasiparticles. As we expect from the theoretical calculations of Ref. 3 and the estimates (2.4)–(2.6) and (2.10), the recombination rate $1/\tau_R$ is the most dominant in the temperature region of interest (above 2.5 K). If the 2Δ-phonon lifetime τ_B is short compared to the τ_R, the relation between τ^* and τ_R is quite simply $\tau^* = \frac{1}{2}\tau_R$. Note that our definition of τ_R follows the one that is customarily used in theoretical calculations: τ_R^{-1} is the rate at which a single quasiparticle recombines. If $\tau_B \gtrsim \tau_R$, one must correct for the fact that at a fraction of time τ_B/τ_R the energy is a 2Δ phonon that does not diffuse, as discussed further in Sec. IV.

The coupled diffusion equations (3.1) are easily solved for a point source by Fourier transforming the equations in time and space and adding a constant source term. The result is

$$\begin{aligned} (iC_e\omega + \kappa_e q^2 + 1/\tau)\tilde{T}_e - (1/\tau)\tilde{T}_p &= A_e , \\ -(1/\tau)\tilde{T}_e + (iC_p\omega + \kappa_p q^2 + 1/\tau)\tilde{T}_p &= A_p , \end{aligned} \tag{3.10}$$

where $\tilde{T}$ denotes Fourier components in the expansion of T in plane waves $e^{i(\vec{q}\cdot\vec{r} + \omega t)}$. The constants A_e and A_p represent a source term appropriate to a δ-function source in space and time.

In the situation of experimental interest, $\kappa_p \ll \kappa_e$ and $C_e \ll C_p$, the eigenfrequencies of (3.10) are

$$\omega = \begin{cases} \omega_+ \\ \omega_- \end{cases} , \tag{3.11}$$

where

$$\omega_+ = i\left(\frac{1}{C_e\tau} + D_e q^2\right) - iDq^2 \frac{1}{1 + q^2/q_C^2} \tag{3.12}$$

and

$$\omega_- = iDq^2/(1 + q^2/q_C^2) , \tag{3.13}$$

where the wave number q_C is defined as

$$q_C = (D_e C_e \tau)^{-1/2} = (D_e \tau_e)^{-1/2} . \tag{3.14}$$

Note that both frequencies are purely imaginary and exhibit a mixture of diffusion and relaxation behavior.

In order to calculate the relative weight of these two modes, we must specify the nature of the source term. We shall assume that $A_e/A_p = C_e/C_p$, corresponding to a heat source at a given temperature. Then it is straightforward to solve (3.10) for the quasiparticle Fourier component $\tilde{T}_e$. Within an arbitrary normalization factor, we get

$$\tilde{T}_e = F/i(\omega - \omega_-) + G/i(\omega - \omega_+) , \tag{3.15}$$

where

$$F = q^2/(q^2 + q_C^2) \tag{3.16}$$

and

$$G = 1 - F = q_C^2/(q^2 + q_C^2) . \tag{3.17}$$

Having obtained the Fourier components $\tilde{T}_e$, we can readily find the form of $T_e(\vec{r}, t)$ itself by integration over momentum and frequency variables:

$$T_e(\vec{r},t)=\int\frac{d\omega}{2\pi}\int\frac{d\vec{q}}{(2\pi)^3}e^{i\omega t}e^{i\vec{q}\cdot\vec{r}}\tilde{T}_e(\vec{q},\omega)$$

$$\propto\frac{1}{r^3}\int_0^\infty u\sin u\left(\frac{\alpha^2}{u^2+\alpha^2}e^{-(u^2Dt/r^2)}+\frac{u^2}{u^2+\alpha^2}e^{-u^2D_et/r^2}e^{-t/\tau_e}\right)du\,, \tag{3.18}$$

since to a good approximation $\omega_-\simeq iDq^2$. We have introduced the important dimensionless variable α through the relation

$$\alpha=rq_C=r/\sqrt{D_e\tau_e}\,. \tag{3.19}$$

It is furthermore convenient to use the dimensionless time variables

$$\beta_1=\sqrt{Dt}/r$$

and

$$\beta_2=\sqrt{D_et}/r=(\sqrt{D_e/D})\beta_1 \tag{3.20}$$

when we perform the integral in (3.18). The result is most easily expressed if we define the function

$$\psi(\alpha,\beta)\equiv\int_0^\infty u\sin u e^{-u^2\beta^2}\frac{\alpha^2}{u^2+\alpha^2}\,du$$

$$=\alpha^2(\tfrac{1}{4}\pi)e^{\beta^2\alpha^2}[e^{\alpha}\Phi(\alpha\beta+1/2\beta)-e^{-\alpha}\Phi$$

$$\times(\alpha\beta-1/2\beta)-2\sinh\alpha]\,, \tag{3.21}$$

where Φ is the error function

$$\Phi(y)=\frac{2}{\sqrt{\pi}}\int_0^y e^{-x^2}dx\,. \tag{3.22}$$

The final result is then seen to be

$$T_e(r,t)\propto\psi(\alpha,\beta_1)+e^{-\alpha^2\beta_1^2}[(\sqrt{\pi}/4\beta_2^3)e^{-1/4\beta_2^2}$$

$$-\psi(\alpha,\beta_2)]\,. \tag{3.23}$$

When plotted for a fixed distance r, the time dependence of (3.23) is characteristic of diffusion. The arrival time of the peak of the pulse depends, however, on the parameter α. Rather than discussing the two limits $\alpha\ll1$ and $\alpha\gg1$ directly from (3.23), we may return to (3.18). In the limit $\alpha\gg1$ we evidently only get a contribution from the first term in the integral characterized by the diffusion coefficient D. In this limit we obtain the usual result

$$T_e(r,t)\propto(\sqrt{\pi}/4\beta_1^3)e^{-1/4\beta_1^2} \tag{3.24}$$

for diffusion from a point source. The time of arrival of the peak is given by

$$\beta_1^2=\tfrac{1}{6}$$

or

$$t=\tfrac{1}{6}r^2/D\,. \tag{3.25}$$

In order to extract D from the measured pulse, it is useful to consider the point of intersection of the tangent at the steepest point on the leading edge with the time axis. This defined the time t given by

$$t=0.0375(r^2/D)\,. \tag{3.26}$$

Physically, the condition $\alpha\gg1$ corresponds to the quasiparticle number decay time τ_e being much less than the arrival time $\sim r^2/D_e$ for a pure quasiparticle pulse. As a result, the combined gas of quasiparticles and phonons travel together in a single pulse characterized by the diffusion coefficient D and the arrival time (3.25). In the opposite limit, $\alpha\ll1$, the quasiparticles and the phonons are no longer in equilibrium because the number decay time is much longer than the pulse arrival time. In this limit only the second term in (3.18) contributes to T_e with the result

$$T_e(r,t)\propto\left(\frac{\sqrt{\pi}}{4\beta_2^3}e^{-1/4\beta_2^2}e^{-t/\tau_e}\right). \tag{3.27}$$

In this limit the arrival time is

$$t=\tfrac{1}{6}r^2/D_e\,, \tag{3.28}$$

which is considerably shorter than (3.25) since $D_e\gg D$.

Finally, to more adequately describe the experimental situation, the solution for an infinite medium may be readily taken over to a finite slab of thickness l with the inclusion of boundary conditions that correspond to zero currents through the surface. The result for the temperature at a point directly across the slab from the heat pulse is

$$T_e(t)\propto\sum_{n=0}^{\infty}(-1)^n[e^{-(n\pi/l)^2D_et}e^{-t/\tau_e}I_n(t/\tau_e)$$

$$+e^{-(n\pi/l)^2Dt}J_n(t/\tau_e)]\,, \tag{3.29}$$

where I_n and J_n can be written in terms of exponential integrals

$$I_n=(1/4\pi D_e\tau_e)[\tau_e/t+e^x\,\mathrm{Ei}(-x)]\,,$$

where

$$x=[1+(\pi n/l)^2D_e\tau_e](t/\tau_e)$$

and

$$J_n=(1/4\pi D_e\tau_e)[e^y\,\mathrm{Ei}(-y)]\,.$$

Here $y=(D/D_e)x$ and Ei is the the exponential-integral function.[7] It is this expression (3.29) that we will compare with our experiments.

IV. EXPERIMENTAL TECHNIQUES

The experiments were performed on high-purity (99.9999%) Pb single crystals obtained from United Mineral and Chemical Corp. The propagation direction was the (111) axis and thicknesses of 4.5, 2.2, 1.67, and 0.87 mm were studied. The crystals could be considered to be infinite slabs, as the transverse dimensions were always very much larger than the thickness. For the thin sample, the propagation length and direction could also be altered by varying the position of the excitation relative to the detector. The resistance ratio $R_{300\ \mathrm{K}}/R_{2\ \mathrm{K}}$ of the thinnest sample was measured to be 20 000. Considerable variations in the measured impurity scattering time (almost a factor of 10; see later) was observed between the 0.87 and 2 mm samples. The samples were polished using a combined mechanical and chemical technique. Great care was taken during this process to avoid straining the crystal and to obtain a relatively smooth surface for the evaporation of the thin-film detectors.

Two types of detectors were used in this study. Superconducting Pb-oxide-Pb tunnel junctions were used to detect the quasiparticles, while superconducting thin-film bolometers were used for, below gap frequency, phonon detection. The Pb junction was prepared directly on the sample in the following way. One surface of the sample was cleaned by back sputtering in argon to remove undesirable surface contaminants. This was done to ensure that we have a true quasiparticle detector. A controlled oxide layer was then grown on this surface, and after suitable insulating masks were deposited, a thin-lead-film stripe was evaporated on top to form the tunnel junction. The procedure for growth of the controlled oxide has been described by Garno.[8] High-quality junctions, with normal-state resistance of 20–50 mΩ and area $\sim 0.25 \times 0.45$ mm^2 were formed. The low resistance and small area ensured that the junction RC time constant was less than 10 nsec. Silicon oxide and photoresist were used to insulate the lead film from the lead crystal outside the junction area. Flexible aluminum foil leads were used to make four terminal electrical contacts with the junction.

The superconducting bolometers used were all of the granular type. They were either Al ($T_c \sim 2$ K), gallium ($T_c \sim 6.5$ K) or $Pb_{1-x}Bi_x$ alloy ($T_c \sim 9$ K, $x \sim 0.25$–0.5). The latter alloy's high T_c enabled us to study diffusive heat transport to temperatures well above the T_c of pure lead. Most of the measurements reported in this paper were made with this latter bolometer, which was fabricated in a highly oxidizing atmosphere (2×10^{-5}–5×10^{-4} Torr of O_2), so that a broad resistive transition that could be tuned conveniently with bias current all the way down to 1 K was obtained. As far as we know, such *granular* Pb:Bi bolometers have not been fabricated before. Unlike the case of tunnel junctions, the bolometers were, of course, electrically insulated from the Pb crystal by means of a 500-Å SiO film. It is important to emphasize that these two different kinds of detectors are sensitive to different excitations. The tunnel junction detects a deviation from equilibrium in the quasiparticle gas but is insensitive to phonons (of energy $< 2\Delta$). The bolometer, on the one hand, is electrically insulated from the crystal and is sensitive only to phonons. These differences will be apparent in the low-temperature data. At higher temperatures, where the diffusion is in the combined gas of quasiparticles and phonons, the detected pulses are similar.

The quasiparticles and phonons were generated on the face opposite to the detector by means of a dye laser that was, in turn, pumped by a nitrogen laser. The laser had a peak power of ~1 kW (only a fraction of which was absorbed by the crystal) with a rise time of 1.5 nsec and a pulse width of 5 nsec. The beam was about 0.2 mm in diameter. The laser and power supply were located outside a shielded room in which the cryostat was placed to eliminate undesirable electrical pickup. Great care was also taken to eliminate scattered light from reaching the detector. The voltage signals from the tunnel detector (biased in the region of thermal quasiparticle tunneling) or the bolometer (biased near its resistive transition were amplified by means of a B & H amplifier with 2-GHz bandwidth. This amplifier had a low frequency rolloff ~100 kHz. This low-frequency rolloff distorted the pulse shape for times greater than about 5–10 μsec. Some data were also taken with a Tektronix 1121 amplifier with a bandwidth of 17 MHz–5 Hz. The high-temperature fits described later were on data obtained with the Tektronix amplifier. The amplified signals were fed into a Biomation 8100 transient recorder with 10-nsec resolution and a Nicolet signal averager. Most of the data was taken with the sample immersed in liquid helium or by cooling in the vapor. No unusual changes were observed in going through the λ point or with the sample in the vapor. We do not expect any influence from the helium, as the thermal conductance of the lead is very much greater than that into the helium. It is a good assumption for calculational purposes that there is no heat flow across the boundaries, and the sample cools by transverse conduction in the slab.

V. EXPERIMENTAL RESULTS

Figure 1 shows some typical pulses observed at high temperatures (between 3.34 and 6.84 K) ob-

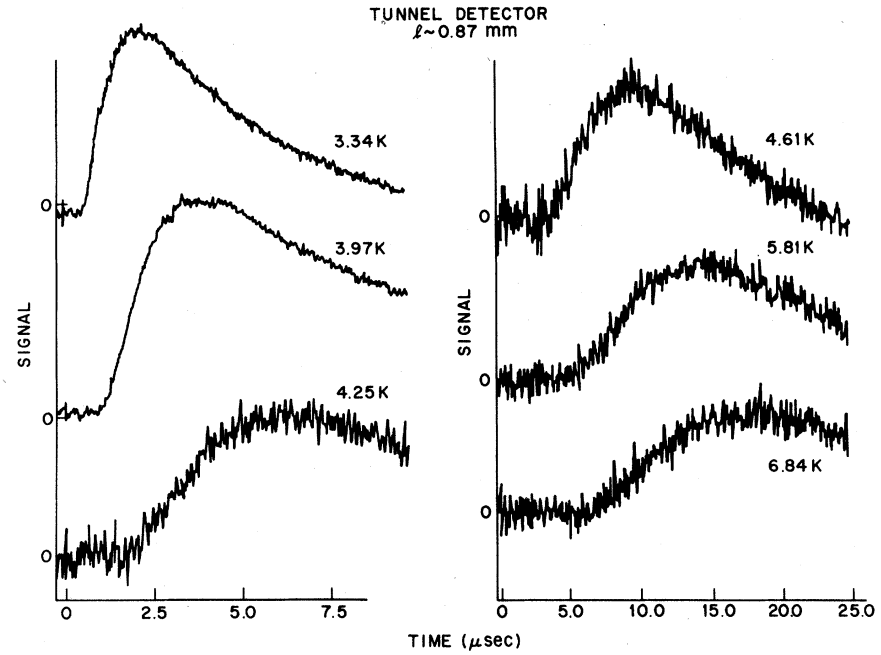

FIG. 1. Quasiparticle signal as a function of time in the high-temperature regime. Tunnel junction detector. The propagation length is 0.87 mm.

served with the tunnel detector and the 0.87-mm sample. The leading-edge arrival times move markedly with temperature and reflect the strong changes in scattering time with temperature (see discussion below). The trailing edge of the high-temperature pulses is somewhat affected by the B & H amplifier rolloff that was used to obtain these data. Later data obtained with a Pb:Bi bolometer at high temperatures showed essentially the same temperature dependence. These data were extended beyond the T_c (7.2 K) of lead, and showed that the diffusive heat transport also occurred in the normal state with no abrupt change at T_c. The arrival time for the pulse in these high-temperature data was found to scale with l^2 as expected for diffusive heat transport.

Unlike the high-temperature data, the data below about 3 K were found to depend sensitively on the nature of the detector. Figure 2 shows some typical data obtained with the quasiparticle detector for $l = 0.87$ mm. At 2.6 K a new pulse is seen to split off from the diffusive heat pulse. This new pulse was found to grow in intensity as the temperature was lowered further. The leading edge of this pulse had a risetime of the order of 100 nsec and an exponentially decaying tail. The peak arrival time of this pulse was found to scale somewhat more slowly than l^2 approaching an l dependence. The line shape of this pulse (as we shall see below) can, however, be fit rather well with a diffusion analysis, and is to be identified with a pulse of diffusing quasiparticles. Below $T \leq 2$ K only the quasiparticle pulse remains.

In Fig. 3 we show data at low temperatures of the quasiparticle pulse for the $l = 2.2$-mm sample. The tail of the quasiparticle pulse between 1.3 and 2.0 K can be seen to depend strongly on the temperature. This is seen clearly in Fig. 4, where

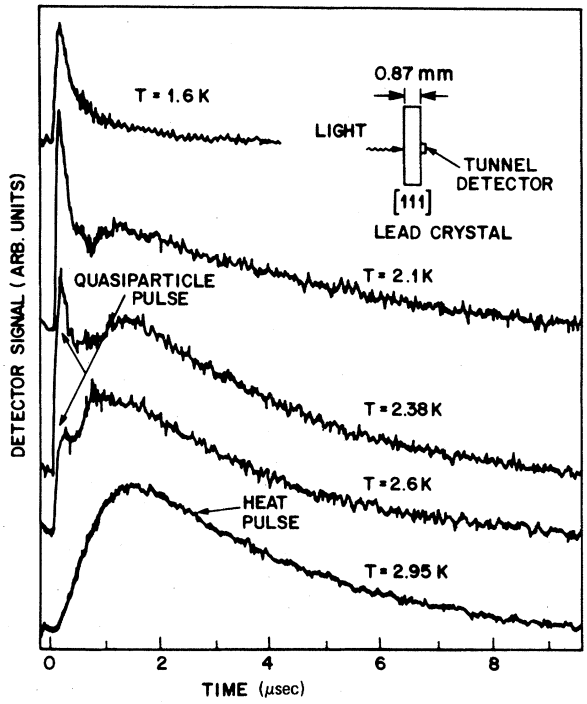

FIG. 2. Temperature dependence (below 2.95 K) of detector signal as a function of time. Tunnel junction detector. The propagation length is 0.87 mm. A true *quasiparticle* pulse splits off from the heat pulse at $T \lesssim 2.6$ K.

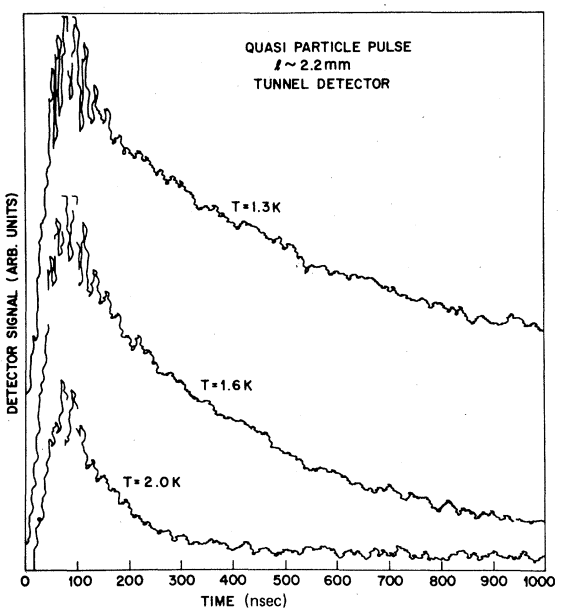

FIG. 3. Low-temperature behavior of quasiparticle pulse as a function of time. Tunnel junction detector. The propagation length is ~2.2 mm.

we have plotted the signal amplitude, beyond the peak, semilogarithmically as a function of temperature. It is clear that the time constant changes by nearly an order of magnitude between 1.2 and 2.1 K.

In Fig. 5 we show the data obtained at $T < 2.55$ K with a Pb:Bi bolometer. The sample was the same as that used in Fig. 3, but with a somewhat reduced

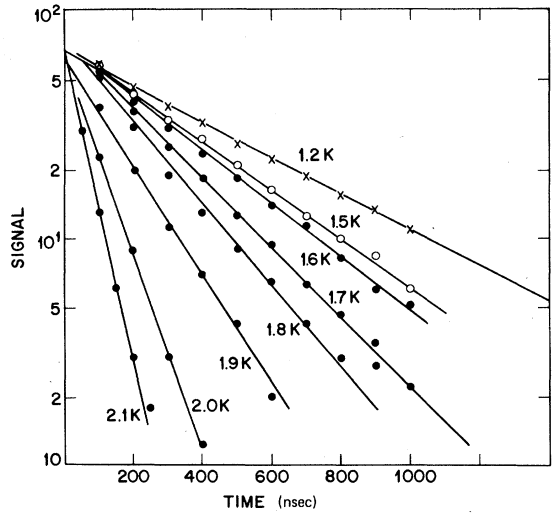

FIG. 4. Semilog plot of the tail of the quasiparticle pulse (see Fig. 3) as a function of time for several different temperatures. Note the large change in slope between 1.2 K and 2.1 K.

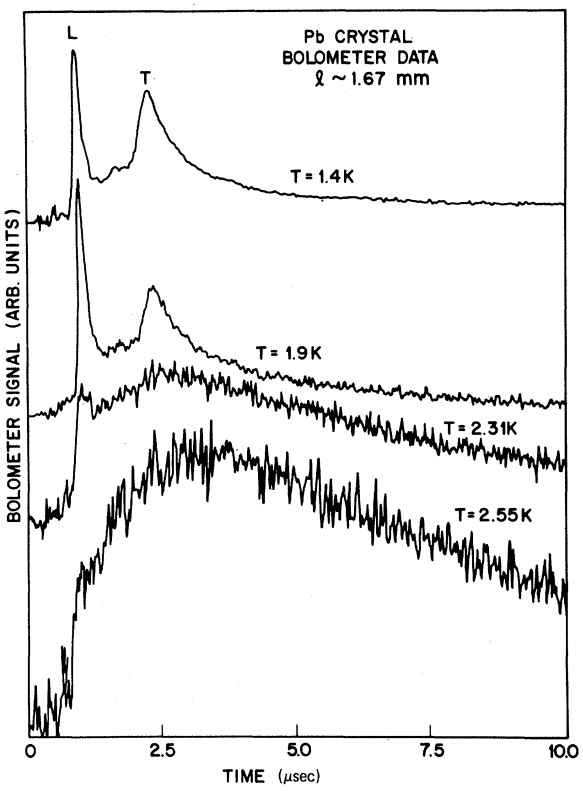

FIG. 5. Bolometer signal as a function of time for four different temperatures. The propagation length is 1.67 mm.

length of 1.67 mm. In contrast to the tunnel-junction data, we now see ballistic phonon pulses (longitudinal and transverse) split off from the diffusive heat pulse as the temperature is lowered below 2.3 K. At 1.4 K we see excellent ballistic phonon pulses whose leading-edge arrival times are now more than an order of magnitude slower than the low-temperature quasiparticle pulse observed with the tunnel detector. In fact, the arrival times are now in excellent agreement with the known sound velocities in lead.

VI. DISCUSSION

A. High-temperature data

Above about 3 K, it is clear that a single diffusive pulse, characterized by a single diffusion constant D, is observed with both the quasiparticle and phonon detectors. This is consistent with the expected extremely rapid scattering between the quasiparticle and phonon excitations of the system estimated from Sec. II. This rapid scattering implies that there is true *local* temperature equilibration between the quasiparticle and phonon gases.

In Fig. 6 we show a detailed line-shape fit to the

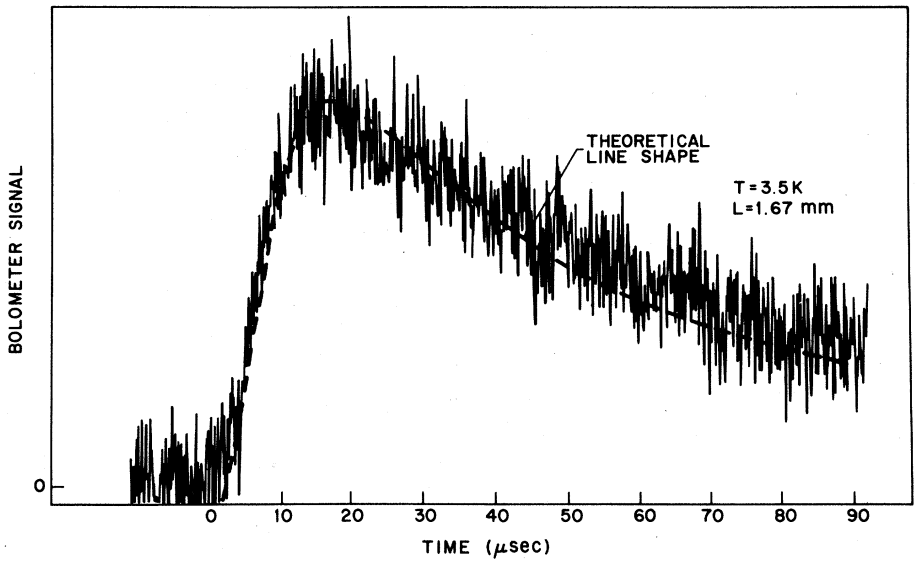

FIG. 6. Bolometer signal as a function of time. $T = 3.5$ K. Propagation length is 1.67 mm. The dashed line is a theoretical fit to the diffusion heat pulse shape. Parameters used are discussed in the text.

diffusion Eq. (3.29) for data obtained with the Pb:Bi bolometer at 3.5 K. From the theoretical curve a value of D was obtained. By including strong-coupling corrections, the specific-heat ratio C_e/C_p is found to be $\sim 0.222 \times 10^{-1}$ at 3.5 K and the thermal quasiparticle velocity $\sim 4 \times 10^7$ cm/sec. This velocity was also calculated from BCS theory with strong-coupling corrections and assuming that the Fermi velocity in lead, $\langle v_F^2 \rangle^{1/2}$, is 1×10^8 cm/sec. This choice appears to be a reasonable mean of the values measured for different orientations by Lykken *et al.*[9] The theoretical fit corresponds to a value of $\tau_e \sim 8 \times 10^{-11}$ sec.

It is important to point out here that the trailing edge of the pulse in Fig. 6 arises primarily from conduction (quasiparticle out diffusion) away from the direction of propagation due to the point nature of the source and detector. This picture is consistent with the negligible effect we observed experimentally of the cooling medium (helium) in determining the line shapes, and is also consistent with the high thermal conductivity of lead.

Fom Eq. (2.6), we determine that the strongest scattering process is recombination, and so we anticipate that our estimates of τ_e are directly related to τ_R. Because two quasiparticles are involved in the recombination process, in Fig. 7 we show a plot of twice the measured scattering time, $2\tau_e$, as a function of temperature. Between 3 and 3.5 K, τ_e was obtained from detailed line-shape fits as described above. At higher temperatures, the leading-edge analysis, (3.26), which gives satisfactory results in the strongly diffusive regime, was used. It is clear from Fig. 7 that the measured scattering time changes by nearly three orders of magnitude between 7 and 3 K. The measured scattering (diffusion) time is particularly short at high temperatures, having values $\sim 7 \times 10^{-13}$ sec near 6.8 K.

The observed magnitudes and the temperature dependence can be quantitatively explained as follows. In lead the shortest scattering time at $T \gtrsim 3$ K is the recombination time τ_R, which depends exponentially on Δ/kT. However, the phonon-pair-breaking time[3] τ_B (at 2Δ) is $\sim 3 \times 10^{-11}$ sec at $T \sim 3$

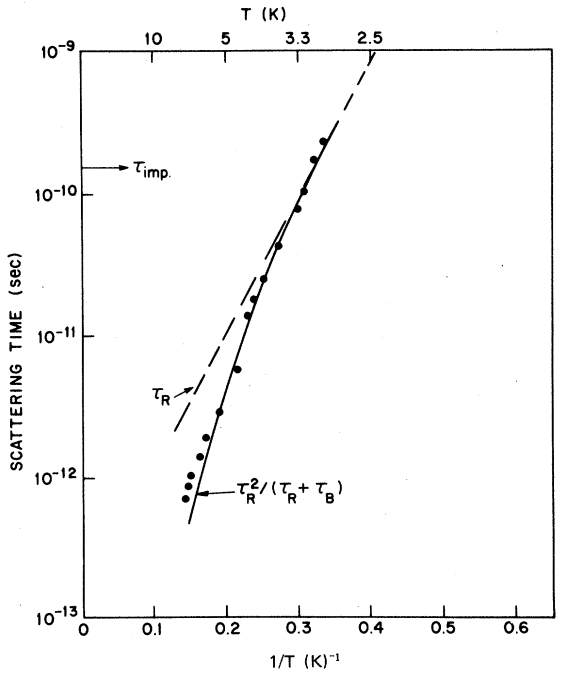

FIG. 7. Semilog plot of twice the measured scattering time (solid circles) as a function T^{-1}. The dashed line is the theoretical quasiparticle recombination time τ_R, while the solid line corresponds to $\tau_R^2/(\tau_R + \tau_B)$, where τ_B is the pair-breaking time in Pb.

K. The pair-breaking time (which is relatively temperature insensitive) becomes comparable to τ_R at $T \sim 3.5$ K. At higher temperatures, especially above 4 K, τ_R becomes much shorter than τ_B. This implies that the observed quasiparticle diffusion is *slowed* down by the ratio $\tau_R/(\tau_R+\tau_B)$, since the energy involved in a recombination process spends a considerable fraction of time as a phonon and not as two quasiparticles. Thus the measured scattering time τ_{meas} is related to τ_R by

$$1/\tau_{meas} = (1/\tau_R)(1+\tau_B/\tau_R) .$$

The solid line is the calculated value of $\tau_R^2/(\tau_R+\tau_B)$ as a function of temperature from the theoretical calculations of Kaplan *et al.*[3] Theory and experiment are in excellent agreement, and our data provide a quantitative measure of τ_R. Figure 8 shows a plot of τ_R determined after making the above corrections, and shows clearly the excellent agreement between theory and experiment. For most superconductors, this correction of τ_B/τ_R is small as τ_R is usually $>\tau_B$. In a strong-coupled superconductor like lead, however, above 4 K this term dominates and the thermal diffusion is substantially retarded by this effect. It is also interesting to note that the results of Fig. 8 suggest that τ_R is sufficiently short so that lifetime broadening effects should be apparent. In a recent tunneling experiment these effects have been directly observed.[10]

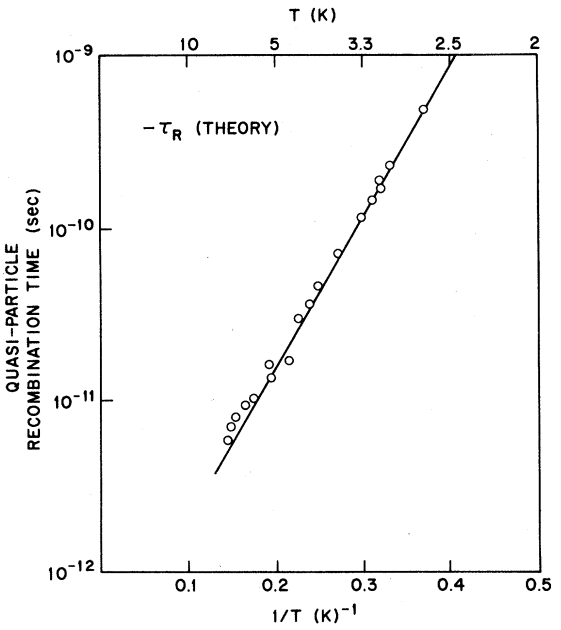

FIG. 8. Quasiparticle recombination time (open circles) calculated from the measured scattering time of Fig. 7. The solid line is the theoretical recombination time τ_R [$\Delta(T=0)$].

B. Transition region

So far we have been assuming that the quasiparticles and the phonons are in equilibrium, so that a local temperature and a single diffusion equation describes the propagation. As discussed in Sec. II at $T \sim 2.7$ K, τ_R becomes long and from the estimates (see Sec. II) the relaxation time τ_{eff} for the quasiparticle number becomes long. Thus in the transition region we really have three pulses propagating: these are the quasiparticle pulse, a phonon pulse, and the remnants of the heat pulse. The heat pulse is detected both by the tunnel junction and by the bolometer, while the quasiparticle and phonon pulses are detected, respectively, by the tunnel junction and bolometer. Furthermore, the quasiparticles (see below) and the heat pulse can be described by diffusion equations for the quasiparticle number and the *local* temperature, respectively, but the ballistic phonons cannot. For this reason, we do not attempt quantitative fits to the data in the transition region. However, in Fig. 9, we show some typical theoretical line shapes for the coupled diffusion equations appropriate for $T = 2.4$ K. In this transition region, we believe quasiparticle scattering time τ_e is dominated by the number decay time τ_{eff}. The values

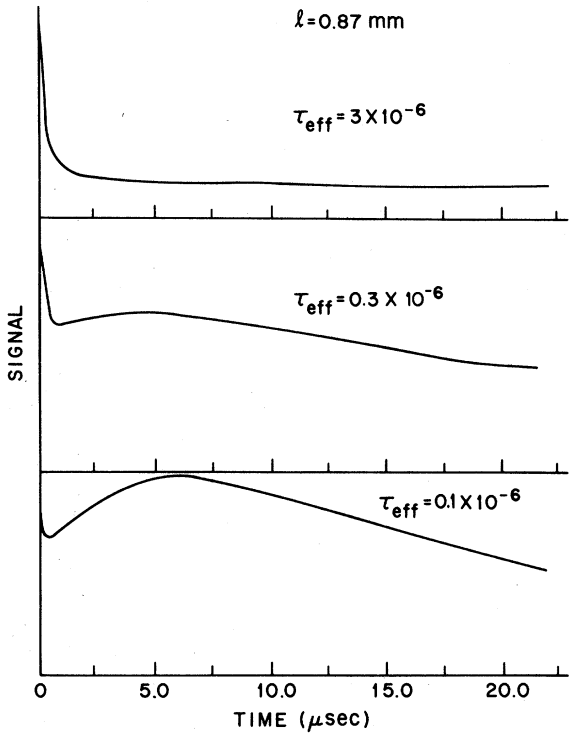

FIG. 9. Theoretically expected line shapes in the transition region. The line shapes were calculated from the coupled diffusion equations [see Eq. (3.29) of text] for three different values of the number decay time τ_{eff}.

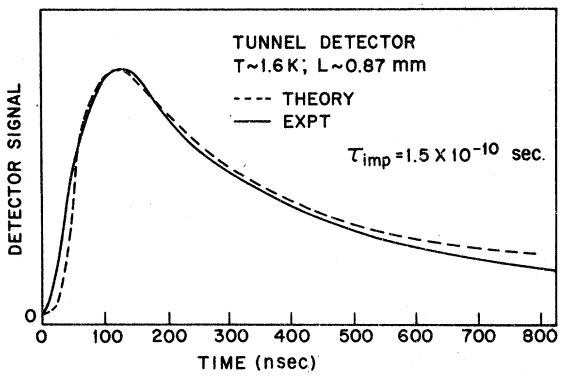

FIG. 10. Low-temperature quasiparticle pulse. T ~1.6 K. The propagation length is 0.87 mm. Tunnel junction detector. The solid line is the experimental data, while the dashed line is obtained from the theoretical diffusion equation with a value of the impurity scattering time τ_{imp} ~1.5×10^{-10} sec.

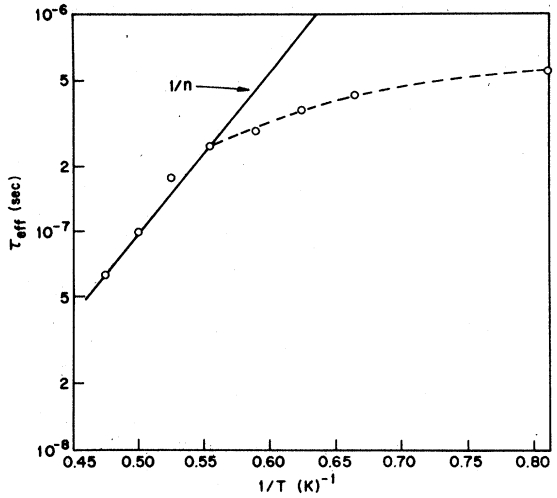

FIG. 11. Semilog plot of the quasiparticle number decay time τ_{eff} vs $1/T$. Open circles obtained from data are shown in Fig. 4. The solid line corresponds to the expected $1/n$ dependence of τ_{eff} .

obtained for τ_{eff} range from about 10^{-6} to 10^{-7} sec. It is clear that in the region of $\tau_{eff}\sim10^{-7}$ sec there are two diffusion pulses reflecting the decoupling of the quasiparticle number with the local temperature as is qualitatively observed with the tunnel detector. Note that the actual arrival time of the second pulse at $T\sim2.5$ K is close to the sound velocity. Thus the neglect of the ballistic nature of the phonons in the transition region is not justified. To make quantitative fits would require a proper treatment of the ballistic phonons, and that is beyond the scope of this paper. We, therefore, choose to obtain more quantitative information of the number decay time τ_{eff} through a study of the tails of the quasiparticle diffusive pulse at low temperatures, as discussed below.

C. Low temperature quasiparticle diffusion

Figure 10 shows an expanded trace of the low-temperature ($T\sim1.6$ K) pulse observed in the 0.87-mm-thick sample. This pulse shape can be quantitatively fit by the diffusion equation with a value of $\tau_{imp}\sim1.5\times10^{-10}$ sec and long-number decay times ($\tau_{eff}\gtrsim10^{-7}$ sec). This fit, then confirms our earlier conjecture that the decoupling between the quasiparticles and the local temperature is now complete with the quasiparticle number diffusion being limited by the impurity scattering.

These ideas are further substantiated by the data on the 2.2-mm sample that we showed in Figs. 3 and 4. In this sample $\tau_{imp}\sim\times10^{-9}$ sec (about one order of magnitude longer than in the 0.87-mm sample). At $T\approx2.1$ K the measured number decay time ~6.3×10^{-8} sec is about one order of magnitude larger than τ_R as expected (see earlier discussion, Sec. II). This time increases inversely proportional to the quasiparticle number density down to temperatures as low as about 1.7 K and provides confirmation of our model. These decay times are plotted in Fig. 11. At the lowest temperatures (1.3–1.6 K) the increase in τ is somewhat slower than expected, but this is almost certainly due to the inevitable *overinjection* of quasiparticles compared to the thermal number. This overinjection becomes more important the lower the temperature.

VII. SUMMARY

In summary, we have studied the propagation characteristics of quasiparticles and phonons in bulk superconducting lead by means of tunnel and bolometric detectors and time-of-flight techniques. The most interesting feature of the data is the observed transition in the pulse propagation from purely quasiparticle (and ballistic phonon) propagation to a diffusive heat pulse in the combined gas of excitations. The data allow a numerical determination of the recombination time τ_R, the number decay time τ_{eff}, and the phonon-pair-breaking time τ_B through detailed line-shape fits of the observed diffusive pulses.

ACKNOWLEDGMENTS

It is a pleasure to thank the following people whose skill and effort have made this work possible. J. P. Garno prepared the single-crystal samples, the bolometers, and tunnel junction, M. A. Chin contributed to the data-taking efforts, and U. Gibson developed the Ga bolometers and contributed to the data collection.

*Present Address: H. C. Ørsted Institute, University of Copenhagen, Copenhagen, Denmark.

[1]For a general review, see D. N. Langenberg, in *Proceedings of 14th International Conference on Low Temperature Physics* edited by M. Drusius and M. Vuorio (North-Holland, Amsterdam, 1975), Vol. V, p. 223.

[2]P. Hu, R. C. Dynes, V. Narayanamurti, H. Smith, and W. F. Brinkman, Phys. Rev. Lett. 38, 361 (1977).

[3]S. B. Kaplan, C. C. Chi, D. N. Langenberg, J. J. Chang, S. Jafarey, and D. J. Scalapino, Phys. Rev. B 14, 4854 (1976).

[4]C. J. Pethick, H. Smith, and P. Bhattacharyya, Phys. Rev. B 15, 3384 (1977).

[5]Carl A. Kukkonen and Henrik Smith, Phys. Rev. B 8, 4601 (1973).

[6]V. Narayanamurti, R. C. Dynes, and K. Andres, Phys. Rev. B 11, 2500 (1975).

[7]M. Abramowitz and I. A. Stegun, *Handbook of Mathematical Functions* (Dover, New York, 1965).

[8]J. P. Garno, J. Appl. Phys. 48, 4627 (1977).

[9]G. I. Lykken, A. L. Geiger, K. S. Dy, and E. W. Mitchell, Phys. Rev. B 4, 1523 (1971).

[10]R. C. Dynes, V. Narayanamurti, and J. P. Garno, Phys. Rev. Lett. (to be published).